UNCONVENTIONAL RESOURCES TECHNOLOGY CONFERENCE
FUELED BY SPE • AAPG • SEG

URTeC: 2688826

Pore Pressure and Elastic Moduli Estimation Considerations for a Simplified Geomechanical Model for Unconventional Plays. A case study in the Vaca Muerta Formation.

Sergio Cuervo and Ezequiel Lombardo, Chevron Latin America Business Unit.*

Summary

The correct estimation of elastic properties and stresses from well logs is a critical step in the planning of long reach horizontal wells as well as in the optimization in the design of hydraulic fracturing, two common and challenging tasks in any unconventional play.

The physics of the relationship between stress and strain in porous media is relatively well known. However, the complexity of the tectonic, depositional and diagenetic processes, together with the commonly limited amount of measurements and related available information make the construction of 1D mechanical models a major challenge. Current published models for unconventionals are highly variable, even for the same play. Initial assumptions, such as material isotropy or pore pressure estimation method used, have an important impact on model results.

In this contribution, we are presenting a complete workflow to define and estimate pore pressure, isotropic and anisotropic elastic moduli, poroelastic effects and finally far field stresses from commonly available well logs. TIV anisotropy in the shale intervals, velocity relationship with effective stress, poroelastic effects and tectonic strains are all considered in the building of the model. Tectonic strain and the minimum to maximum tectonic strain ratio were the parameters used for model calibration. Failure analysis and ISIPs, together with triaxial test results were the main sources of calibration for the model.

This case study covers 40 vertical wells with electric, sonic and nuclear logs in a region of the Neuquén basin known as Neuquén Embayment. All the wells in this set are in the oil and condensate windows.

Introduction

The Vaca Muerta formation is a thick lithostratigraphic unit present in a wide area of the Neuquén Basin, located in central west Argentina. From a lithological point of view it is characterized by organic rich carbonatic shales reaching up to 350 m in thickness (Fantin et al, 2014) in the study area (Fig. 1). The exploration stage of the play started in 2010 (Rimedio et al, 2015) and currently there are several hundreds of vertical and horizontal wells drilled within this target.

The Neuquén Basin is filled with siliciclastic, carbonatic and evaporitic sediments deposited during the Jurassic-Cretaceous Interval. Since the late Cretaceous, the basin has been under active tectonic stresses related to the Andean uplift, conditions that continue into the present (Howell et al, 2005). Tectonic compressive pulses in this interval generated uplift and erosion in the basin (Uliana, M. and Legarreta, L., 1993) with the consequent overcompaction as reflected in available porosity and velocity logs. The first-order present-day stress orientation in the basin is mainly controlled by the plate boundary forces. The maximum horizontal stress derived from regionally distributed wellbore breakouts has a preferred trend close to the west-east direction (Guzmán et al, 2007).

As in most unconventional plays the development of Vaca Muerta requires the drilling of long-reach horizontal wells and the use of hydraulic fracturing for completing these wells. Drilling and completing wells in the play has presented several problems, like stuck pipe or mud losses ended up in costly side tracks and occasional influxes that have been

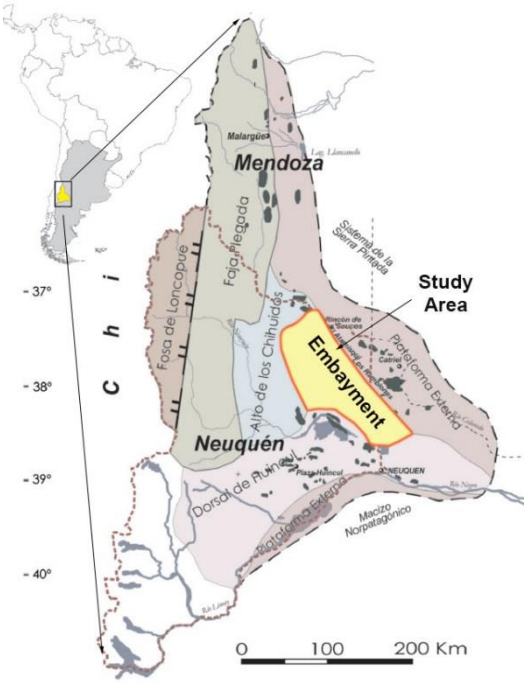

Figure 1: All the wells in the present study are in the area known as the Neuquén Embayment. Fluid type in this area range from early oil to condensate. (modified from Schmidt et al 2014).

experienced by several operators. On the well completion side, sanding and casing deformation after hydraulic fracturing have also been observed in different concessions of the basin. A reliable geomechanical model can help to mitigate these problems and may be an invaluable tool for any production improvement and drilling cost optimization program.

The aim of a geomechanical model consists of the estimation of elastic and strength parameters, pore pressure and, stress orientation and magnitudes from well logs or properties derived from seismic. As commonly happens in most subsurface formation evaluation tasks, the rock physical properties are the result of a complex depositional, diagenetical and structural history and the geophysical measurements available are very limited. As a consequence, after applying physical principles, some correlations and simplifications different assumptions need to be used to solve this model.

The simplest geomechanical model imply a known lithology column of elastic isotropic rocks, hydrostatic pore pressures, a structural history free of uplift and erosion and the absence of tectonic strains. Unfortunately, none of these assumptions are valid in this case study (as in most of the unconventional plays).

The Neuquén Basin of Argentina and central Chile contains a near-continuous Late Triassic-Early Cenozoic succession deposited on the eastern side of the evolving Andean mountain chain. (Howell et al, 2005). The basin has suffered contractional deformation from the Late Cretaceous onwards in several episodes; while the main events took place in the late Miocene with a west-east orientation of the major stress. The Neuquén Embayment (Fig. 1) has a complex structural history with different sectors being deformed and uplifted (Mosquera, A. and Ramos, V. A, 2005). Uplift and erosion generated overcompaction, altering the depth-porosity relationships. If effective stress methods are going to be used for estimating pore pressure, this effect needs to be considered to avoid biased results.

Regarding the elastic properties, for sandstones and carbonate sedimentary sequences, assuming isotropy is usually a good proxy for real rock behavior and is applied by many authors. In laminated and compacted shales, on the other hand, there is evidence of high anisotropy in elastic moduli measured parallel and perpendicular to bedding with differences up to 400% in some extreme cases (Suarez Rivera et al, 2011). Static Young's modulus anisotropy in our triaxial test dataset range between 15 and 250%.

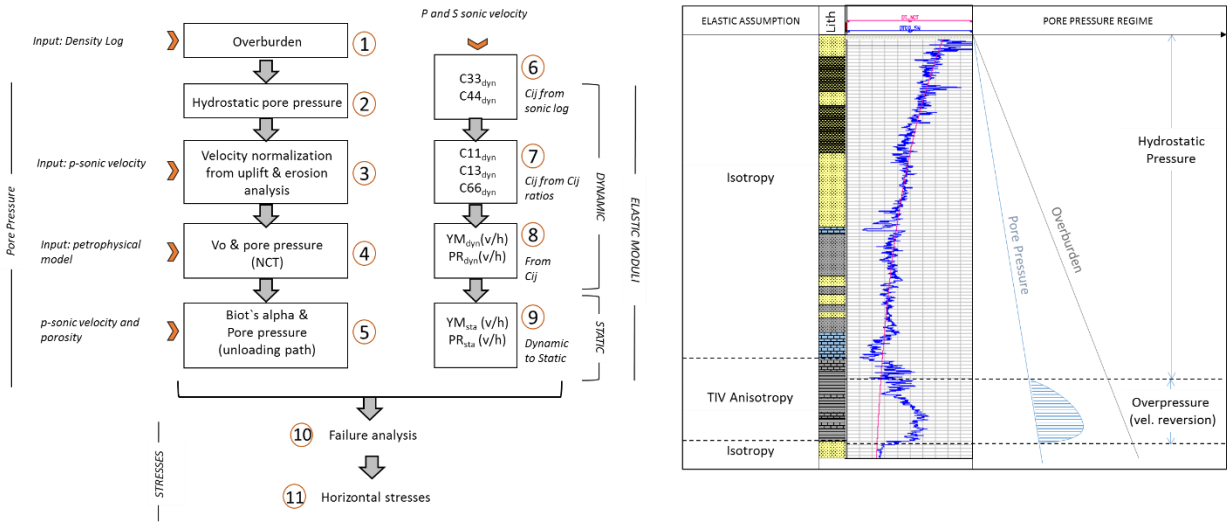

Figure 2: Left: Generalized workflow of the 1D mechanical earth model schematizing inputs, computations and outputs. Right: schematic elastic and pressure regime zones where different assumptions for the computation of the model need to be made.

The Neuquén basin is at present under active tectonic stress. Guzmán et al (2007) in a regional study using borehole breakout analysis estimate a maximum horizontal stress direction of 88.7º (almost west-east) probably associated with plate boundary forces related to the subduction of the Nazca plate. The analysis of our wellbore image database show no vertical stress rotation and in general low breakout angles. It is inferred from our failure models honoring breakout occurrence that horizontal stress anisotropy is high in the study area.
The main objective of the present contribution is to introduce and discuss an integrated and complete workflow (Fig. 2) to estimate far-field stresses from well logs. For the execution of the workflow a petrophysical model is required, a simplified model for estimation of matrix and fluid components from commonly available logs in Vaca Muerta was presented by Cuervo et al (2016) and has been an integral part of the current analysis.
The case study includes 40 vertical wells spread out along the area demarked in Fig. 1. These wells all have at least dipole sonic, density-neutron, gamma ray and resistivity logs available. All the wells were hydraulic fractured at different depths in the Vaca Muerta interval providing ISIPs that were used as upper boundary control for the estimation of the minimum stress. 14 wells had wellbore images, where the failure analysis was calibrated against induced fractures and wellbore breakouts. 8 wells had triaxial test from core plugs, in most cases with measurements parallel and perpendicular to bedding, ultrasonic velocities were also available to generating ad-hoc dynamic to static conversions.

Background, Assumptions and Initial Considerations

Pore Pressure

Hydrostatic pore pressure is generated in all the sedimentary basins as a consequence of the pressure exerted by the column of fluid from the water table to a specific depth. Overpressure is the term used by the industry for zones where the pressure is higher than the hydrostatic. The sources of overpressure have been studied by different authors, and a good compilation of the existing theories can be found in the AAPG Memoir 76 (Huffman, A. and Bowers, G. Ed., 2001). Pore pressure is one of the most impactful variables for the estimation of far field stresses (Fig. 3). The main source of overpressure identified in the literature is the disequilibrium compaction generated when the sedimentation rate is higher than the rate at which the water is expelled from the pore space during normal compaction (common in basins with high rate of sedimentation like the Gulf of Mexico). It is described by Swarbrick et al (2011) that deposition rates during the deposition of the Vaca Muerta-Quintuco system are significantly lower than the rates reported for the Gulf of Mexico and therefore this mechanism is not believed to be the source of overpressure in Vaca Muerta. When disequilibrium compaction is the generator of overpressures the onset of the overpressures is independent of the amount of organic carbon present in the rock. This is not the case in Vaca Muerta.
Other source of overpressure identified as important by some authors (Sayers et al, 2010) is the clay diagenesis, specifically the smectite to illite conversion (Hower et al, 1976). Quantitative X-Ray diffraction analysis ran in cutting and core samples taken above and below the onset of the overpressures in Vaca Muerta do not show the expected changes in the Illite/Smectite ratios reported in other basins in association with changes in pore pressure regimes.

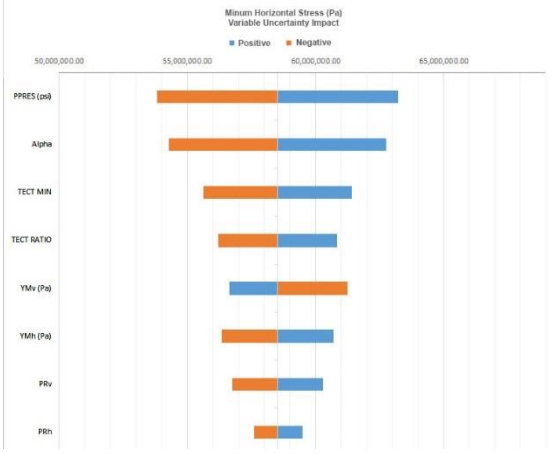

Figure 3: Tornado plot showing the impact on the estimated stress of each variable considering uncertainties estimated from common estimation methods for each. Note the impact of pore pressure estimation in the stress estimation.

Finally, a well-known source of overpressure in fine sediments is fluid expansion by thermal cracking. The conditions needed for this process to occur are a high content of total organic carbon and burial depths with the pressure and temperature needed for kerogen maturation and hydrocarbon expulsion. The volumetric changes in this transformation depends on several factors, like kerogen type and host rock characteristics, some authors mention it can increase up to 100% of the original volume (Meissner, 1978). In our study case, we have analyzed 40 vertical wells with electric, sonic and nuclear logs. As shown in the example of Fig. 7 in our case the onset of overpressure is accompanied by a reversion in velocity and an increase in the organic matter content.
The method used here for the estimation of the pore pressure is a modification of the Bowers (1995) effective stress method. The concept of effective stress was originally introduced by Terzagui (1936) and implied that the difference between the total stress and the pore pressure ($\sigma' = \sigma - Pp$), rather than the

total stress itself is what determines when a rock fails under external load. This idea was completed by Biot ($\sigma' = \sigma - \alpha \cdot Pp$) to take into account the part of the total stress carried by the solid framework (σ'), the part that is carried by the fluid in the pore space ($\alpha \cdot Pp$) and the remaining pressure that is counteracted by stresses in the solid framework ($Pp\ (1-\alpha)$), (Fjaer et al, 2008) Being σ: total stress, σ': effective stress, Pp: pore pressure and α: Biot's constant.
In a pioneering work, Bowers (1995) set the base for the computation of overpressure based on effective stress-velocity relations, relating velocity trends to different pore pressure regime and overpressure source mechanisms. Bowers presented the empirical equation for the virgin curve or normal compaction trend (NCT) (Eq. 1) applicable where normal compaction of sediments occurs and stated that the same equation is also applicable for intervals with overpressure generated by disequilibrium compaction (in the intervals where the compaction stops and pore fluid begins to support part of the overburden). For intervals where fluid expansion mechanisms occur, a reversion in the normal compaction trend (reflected in a reversion of velocities) takes place. As the process of porosity loss is not elastic the reversion generated by thermal cracking and subsequent increase in porosity follows a different path, denominated by Bowers as the "unloading path", that is modeled with Eq. 2.

$$Vp = V_0 + A\sigma'^{B} \quad (1)$$

$$Vp = V_0 + A[\sigma_{max}(\frac{\sigma'}{\sigma_{max}})^{\frac{1}{U}}]^{B} \quad (2)$$

Where:

$$\sigma_{max} = (\frac{Vmax - V_0}{A})^{\frac{1}{B}} \quad (3)$$

Where Vp is the compressional velocity, σ the total stress, σ' the effective stress, V_{max} and σ_{max} are the maximum values of velocities and stress above reversion and V_0 is the velocity at zero effective stress, in the Bower's initial equation assumed as 5000 ft/s. A, B are fitting constants.
For the velocity reversion interval Bowers derived the empirical equation (2) and added an additional constant, U, related to the plasticity of the sediment. The method relies on the capability of building a reliable NCT-Velocity function.
There are three main problems affecting the applicability of this method, when used in its original version. Firstly, NCT-Velocity functions are altered by uplift and erosion, thus the use of non-normalized compressional velocities from well logs will overestimate effective stress. Additionally, the eroded thickness varies regionally, so most probably any fitting parameter will only be valid for a small area of the basin. Secondly, the method does not account for lithology and porosity variation that locally modify the NCT-Velocity relation. Thirdly, deriving effective stress from the rest of the variables, even when the value of the total stress is known independently, will yield only the combined effect of pore pressure and Biot's alpha in shale intervals, and not just pore pressure.
For the Vo a sequence of normalization is proposed. The verification method is the comparison of the compressional sonic curve from the well with a synthetic curve that includes all the fitting factors (Fig. 4). This method will be explained here.

Normalizing for overcompaction

Several unconventional plays have experienced uplift and erosion after maximum burial depth. Normal compaction under overburden is seen in shales as an exponential function of porosity with depth that generates an increase in interval velocities. Several simple methods for the determination of the erosion thickness from sonic logs have been published (Magara, 1978, Davine, 2014 and Singh et al, 2016). In this work, we have followed the method described by Singh et al (2016) based on the Athy's (1930) equation.
To estimate the uplift either a theoretical normal compaction curve needs to be used as a reference, or a well in a region without uplift and erosion needs to be used for building the reference NCT.
In our workflow, we have used an available well in the easternmost part of the basin where the erosion is assumed to be very limited and in agreement with published theoretical values for NCT trends (Burrus 1998). The original function for the NCT in the Athy (1930) equation:

$$\varphi = \varphi_0 e^{-\beta\sigma'} \quad (4)$$

Where φ is porosity, φ_0 is initial porosity at zero effective stress, σ' is the effective stress and β is an empirical constant
The method suggested by Singh et al 2016 consists of delineating the shale intervals, estimating sonic porosities with the Wyllie equation and then compare the sonic porosities with the model porosities derived using the Athy equation. As effective stress in normally compacted sediments is easily estimated from depth, the necessary depth shift to match the real and theoretical porosity function will then provide the estimated erosion gap.

The Vo term in Bowers equation for the normal compaction interval (1) is then normalized for erosion with the proposed following equation (A graphical explanation is offered in Fig. 4):

$$Vp = \left(V_0 - V_{0_{ERO}}\right) + A\sigma'^{B} \quad (5)$$

Where Vo is the velocity at zero stress for the non-eroded normal compaction curve, Vo_{ERO} is the velocity at surface for the well in study, σ' is the effective stress, and A and B are the Bower's coefficients for the virgin curve.

Normalizing for matrix and fluid components

Sayers et al (2003) show that in the analysis of empirical correlations between velocity and effective stress, based on the original Bowers relation, additional parameters need to be considered to improve correlation predictability. Therefore, empirical factors for porosity and clay content are introduced in Eq. 6

$$Vp = a_1 - a_2\varphi - a_3V_{Clay} + a_4\sigma'^{B} \quad (6)$$

Where a1, a2, a3, and a4 are fitting coefficients

Most of the unconventional shales have some proportion of carbonate components. In the case of Vaca Muerta, the average carbonate is close to 40%. Another important component in velocities is the kerogen. We propose a more comprehensive equation that considers all the main matrix components as well as the porosity:

$$Vp = A\sigma'^{B} + b_0 + b_{\text{por}}\varphi + b_{carb}V_{carb} + b_{qfm}V_{qfm} + b_{clay}V_{clay} + b_{pyr}V_{pyr} + b_{Ker}V_{ker} \quad (7)$$

Where all b's are correction coefficients by matrix and fluid components multiplying the fraction percentage volume of each component in the rock.

In the normal compaction zone of the well, pore pressure is mainly hydrostatic and effective stress can be independently estimated. In this section, using the previous correction, Vp and Vp synthetic need to match as close as possible. (Fig 7). This provides confidence that the factors for matrix and porosity are correct. In the overpressure interval the effective stress is directly derived from the unloading path replacing (7) in (2) the equation to derive effective stress from compressional velocity proposed here is expressed in (8):

$$Vp = \sum b_iV_i - V_{0_{ERO}} + A\left[\sigma'_{max}\left(\frac{\sigma'}{\sigma'_{max}}\right)^{\frac{1}{U}}\right]^{B} \quad (8)$$

Thus, the main elements affecting the velocity-effective stress relation are accounted for. Using (8) with the adjusted compositional coefficients, with a consistent function for the normal compaction trend and an with an accurate determination of porosity, effective stress can reliably be derived from well log compressional velocities (or seismic interval velocities) in unconventional reservoirs. In our case study, all these variables where solved from standard quad combo suit logs using the integrated formation evaluation workflow described in Cuervo et al (2016).

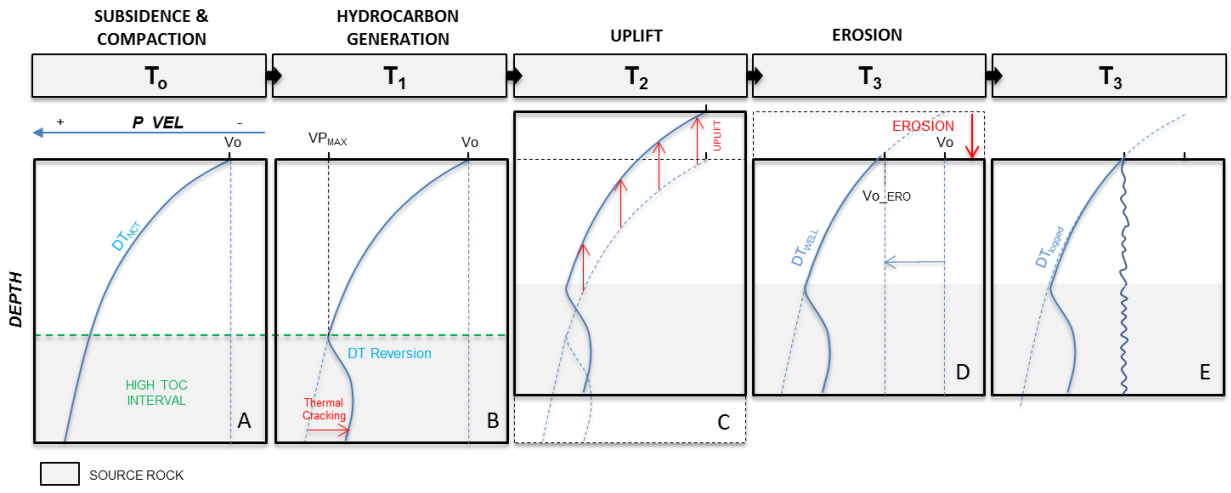

Figure 4: Schematic sequence of stages in the evolution of the study area and its impact on the velocity-effective stress relation, (normalization of the Vo term of the Bowers equation is included). A: representative velocity depth trend for a normal compacted basin when organic rich rocks have not reached the hydrocarbon expulsion maturity window. Organic rich rocks of the Vaca Muerta formation experienced fluid expansion from thermal cracking with associated overpressures and velocity reversion (the thermal maturity time window for Vaca Muerta is estimated for the study area between the Late Cretaceous and the Eocene). C: Uplift, starting in L. Cretaceous but mainly occurring during Miocene. D: Erosion and subsequent overcompaction, Vo normalization needed. E: Velocity normalization for matrix and porosity.

Estimation of Elastic Moduli

To compute stresses, the ultimate objective of any mechanical earth model, the elastic properties of the rocks need to be defined. For an anisotropic material, linear elastic theory defines that each stress component is linearly related to strain components by independent coefficients.

$$\sigma_{ij} = C_{ijkl}\varepsilon_{kl} \quad (9)$$

Where σ_{ij} is the stress tensor, C_{ijkl} is the stiffness tensor consistent of elastic constants and ε_{kl} is the strain tensor.
In the stiffness tensor, the indices i, j, k and l generate 81 different constants. Due to symmetry considerations some of these constants vanish, leaving the number of moduli needed for solving a full anisotropic material to 21 independent constants. Most of the rocks, due to a common depositional and diagentical processes, can be satisfactorily studied assuming some specific symmetries. In marine shales deposited in calm distant bottomsets, where flocculation and authigenic carbonate generation are the main sedimentation mechanisms, assuming similar properties in the paleo-depositional plan makes sense. It can actually be seen in well logs sensitive to horizontal anisotropy, as the dipole sonic log. When rocks have only one direction of anisotropy, this case is called TIV (transversely isotropic vertical) anisotropy, assuming low dipping rocks, where the lamination direction is almost horizontal. Due to this symmetry considerations (see Fjaer et al, 2008 for a detailed explanation) the stiffness tensor, when expressed as a 6 x 6 matrix is reduced to only 5 constants as follow:

$$\begin{bmatrix} C_{11} & C_{11}-2C_{66} & C_{13} & 0 & 0 & 0 \\ C_{11}-2C_{66} & C_{11} & C_{13} & 0 & 0 & 0 \\ C_{13} & C_{13} & C_{33} & 0 & 0 & 0 \\ 0 & 0 & 0 & C_{44} & 0 & 0 \\ 0 & 0 & 0 & 0 & C_{44} & 0 \\ 0 & 0 & 0 & 0 & 0 & C_{66} \end{bmatrix} \quad (10)$$

Where C_{11}, C_{13}, C_{33}, C_{44} and C_{66} are elastic constant that can be measured in triaxial lab tests or be derived from well logs. For isotropic rocks the stiffness tensor can be defined with just two constants (e.g. Young's modulus and Poisson's ratio). In the case of TIV rocks plugs taken parallel, perpendicular and at 45 degrees of the rock lamination will be required for laboratory testing. The computation of the stiffness tensor along a well trajectory is done with the help of well logs, where a dipole sonic and a density log are the minimum requirement. The fundamentals of using sonic and density measurements to calculate elastic properties rely on the wave theory. Elastic waves in rocks propagate with a velocity that is given by elastic stiffness and the density of the rock.
For isotropic rocks, where only two elastic constants are needed the following equations can be used:

$$E = \rho v_s^2 \frac{3v_p^2 - 4v_s^2}{v_p^2 - v_s^2} \quad (11)$$

$$\nu = \frac{v_p^2 - v_s^2}{2(v_p^2 - v_s^2)}$$

Where E is the isotropic Young's modulus and ν is the Poisson's Ratio, v_p and v_s are the compressional and shear velocities respectively.
In the TIV case the constants C_{33} and C_{44} are easily derived from compressional and shear velocities perpendicular to bedding, available from well logs. The estimation of C_{11} and C_{66} are function of compressional and shear velocities parallel to bedding and C_{13} is a function of velocities at 45 degrees of the bedding. For the last three constants C_{11}, C_{66} and C_{13} there is no well log tool that can take this measurements in a vertical well, so the only option for building a TIV model from well logs is using correlations derived from triaxial testing, then:

$$C_{33} = \rho v_p^2 \quad (12)$$
$$C_{44} = \rho v_s^2$$
$$C_{11} = m_1 + m_2 C_{33}$$
$$C_{66} = m_3 + m_4 C_{44}$$
$$C_{13} = m_5 + m_6 C_{33}$$

Where m_{1to6} are fitting factors derived from triaxial test correlations.
Once the 5 independent Cijs for the TIV have been determined, the values for E and ν parallel and perpendicular to the bedding can be computed using the following equations:

$$E_v = \left(\frac{2*C_{13}*C_{13}}{C_{11}+C_{12}}\right) \quad (13)$$

$$E_h = \frac{(C_{11}-C_{12})*(C_{11}C_{33}-2C_{13}C_{13})+C_{12}C_{33}}{C_{11}C33 - C_{13}*C_{13}}$$

$$\nu_v = \frac{C_{13}}{C_{11}+c_{12}}$$

$$\nu_h = \frac{C_{33}C_{12}-C_{13}C_{13}}{C_{11}C_{33}-C_{13}C_{13}}$$

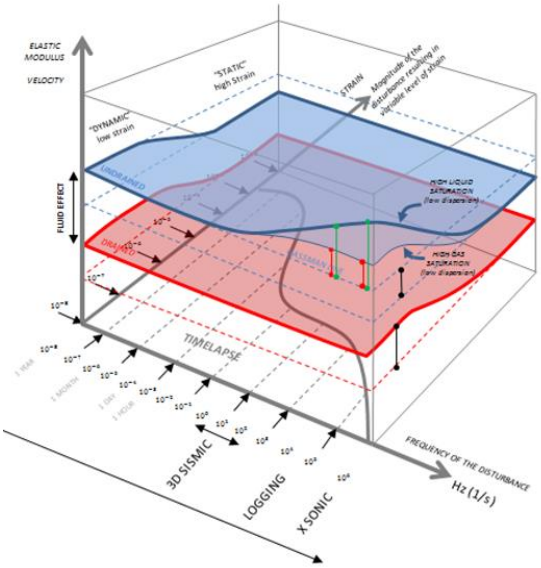

Figure 5: Diagram showing how frequency, liquid saturation and magnitude of the disturbance affect dynamic to static moduli conversion (Luca Duranti, personal communication)

As we mentioned earlier, we use elastic wave theory for computing the stiffness tensor from log velocities. By directly applying the equations derived from wave theory could lead to the conclusion that the elastic moduli determined in triaxial laboratory tests can be directly estimated from velocities obtaining similar values. Unfortunately, this is not the case. Usually the moduli estimated from velocities are larger than the corresponding statics ones (Fjaer et al, 2008). Fjaer postulate as possible causes of this mismatch the effect of the fluids, the effect of velocity dispersion with frequency, the differences in strain magnitudes and grain to grain interactions. For practical purposes, as static values are needed to compute stresses, empirical correlations need to be used. In this contribution, we use empirical linear correlations between dynamic and static moduli derived from correlations from laboratory triaxial tests. Laboratory ultrasonic frequencies are from one to two order of magnitude higher than sonic log tools. Thus, a small mismatch between laboratory velocities and sonic velocities may be observed. In our database, we have seen that average dispersion correction is almost negligible. The general solution for dynamic to static correction then takes the form of:

$$C_{ij\_sta} = c_1 + c_2 C_{ij\_dyn} \qquad (14)$$

Where c_1 and c_2 are fitting empirical constants for each C_{ij}

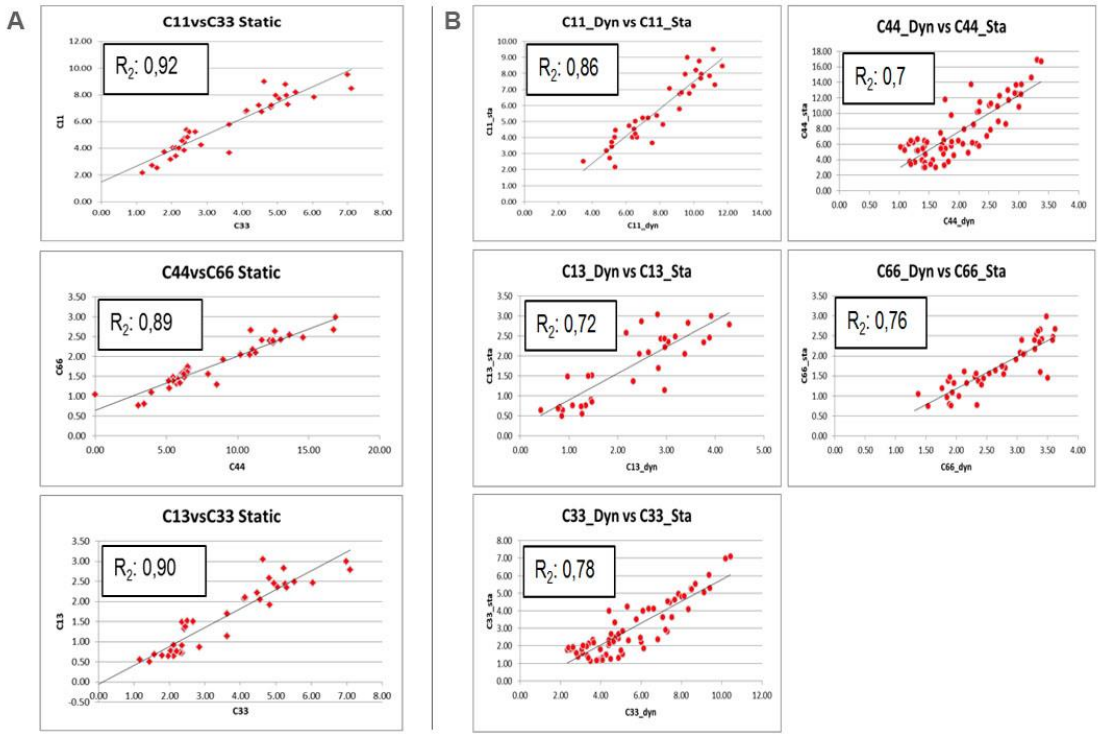

Figure 6: Left: basic correlations used to build the pseudo-TIV model. Samples cover a wide range of depths and come from different regions. Strong correlation coefficients allow estimating C11, C66 and C13 from C33 and C44. Right: dynamic to static correlations extracted from triaxial ultrasonic velocities used in this workflow.

Accounting for poroelasticity and final derivation of pore pressure

Previously, we showed a method to estimate effective stress from compressional velocities correcting for matrix components, porosity and overcompaction. As we are using an effective stress approach, solving (8) for σ' will provide not just pore pressure as in the original Terzaghi (1936) assumption (σ'=σ-Pp), but also the combined effect of Biot's alpha times pore pressure as expressed in the Biot's poroelastic theory, where:

$$Pp = \frac{\sigma - \sigma'}{\alpha} \quad (15)$$

being σ the total stress and σ' the effective stress and α the Biot's coefficient.

For an isotropic material Biot's alpha is a function of the compressibility of the framework and the solid as expressed in Eq. 16.

$$\alpha = 1 - \frac{K_{fr}}{K_s} \quad (16)$$

Where K_{fr} is the drained bulk compressibility modulus of the rock and K_s is the grain compressibility modulus of the matrix at zero porosity.

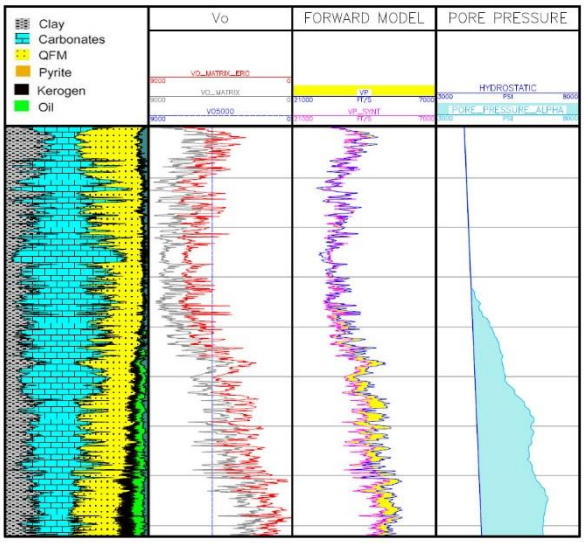

Figure 7: Third track show sonic log P-velocities versus synthetic velocity derived from the application of Eq. 8. It is expected only a good match in the hydrostatic pressures interval. In the overpressure zone differences between both curves are due to the combined effect of pore pressure and Biot's alpha on the velocity curve.

Laboratory determinations of Biot's constant in shales are not very common. Suarez Rivera and Fjaer (2012) published measurements for the Mid-Bossier and Haynesville shales showing values between 0.27 and 0.82. They also showed important differences in shale rocks between the parallel and perpendicular to bedding components of Biot´s alpha. Mitra et al (2016) using a different laboratory design showed values ranging between 0.62 and 0.81 for a Travis Peak formation shale. Grain compressibility is difficult to measure and assumptions from different authors show big differences that will directly impact the estimation of Biot's alpha. Frydman et al (2016) used the grain modulus of calcite (76.8 MPa) for the computation of alpha in a Vaca Muerta shale case study, whereas Mitra et al (2016) estimated a Ks of 47.4 MPa for a generic shale sample. Suarez Rivera and Fjaer (2012) show Ks values between 26.9 and 34.5 GPa in most cases.

For TIV material Biot's alpha can be written for the parallel and perpendicular to bedding component as (Suarez Rivera and Fjaer, 2012):

$$\alpha_v = 1 - \frac{2C_{13}+C_{33}}{3K_s} \quad (17)$$

$$\alpha_h = 1 - \frac{C_{11}+C_{12}+C_{13}}{3K_s}$$

In most shales there are important mineralogical variations in the vertical profile. The same statement is true for the TOC. Solid compressibility between minerals vary a lot, quartz and feldspars, usually an important percentage of the shale assemblage have a Ks around 37.5 GPa, kerogen can reach more than 15% in volume and has a Ks of 2.9 MPa. (Mavko et al, 2009). The average matrix composition in the Vaca Muerta interval (Cuervo et al, 2016) is approximately 40% Clay, 20% Quartz + Feldspar, 25% Clays and 15% Kerogen as volume percentages. Using Mavko et al, 2009 endpoints this composition gives a weighted average of 44.9 GPa for Ks. The Ks assumption has a strong impact in α computation and hence on pore pressure estimation.

In the workflow proposed here, the weighted average method is used taking the reference values for each matrix component from Mavko (2009).

In reservoir engineering applications, the separate value of the pore pressure is indispensable for an accurate dynamic reservoir modeling. As stated in Eq. (15) Biot's alpha is required to obtain this value once the effective stress is estimated.

Stress Estimation

With a gentle topography and a relative "layer cake" stratigraphy free of diapirs, as in our case study, it is safe to assume the principal stresses aligned in the vertical and two defined horizontal directions. The principal vertical stress, normally denominated overburden is calculated from density logs using equation 18. The maximum horizontal stress direction depends on the direction of the tectonic forces and in general can be easily derived from well breakouts or induced fractures observed on wellbore images. The magnitude of the horizontal stresses is a function of the overburden, effective stress, elastic properties and tectonic strains. Equations considering vertical and horizontal components of the poroelastic constant are shown in (19) and (20) (Higgins et al 2008, Suarez Rivera and Fjaer, 2012).

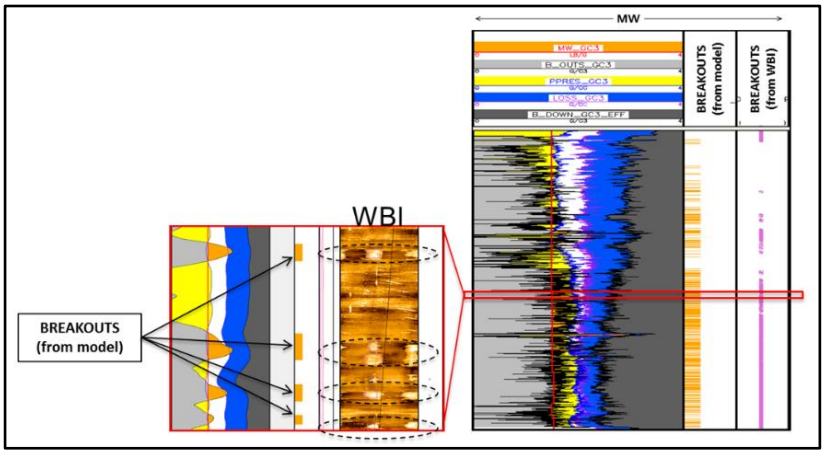

Figure 8: Failure analysis based on Mohr-Coulomb criteria allows the estimation of the shear failure curve (b_out in the chart), usually expressed in mud weight equivalent units. This curve is compared with the mud weight used to drill the well and the concordance between the breakouts observed in wellbore images and the breakouts predicted by the model are used for tectonic strains calibration purposes.

$$\sigma_v = \int_0^z \rho(z) g dz \tag{18}$$

$$\sigma_h = \alpha_h P_p + \frac{E_h}{E_v}\frac{\nu_v}{1-\nu_h}\left(\sigma_v - \alpha_v P_p\right) + \frac{E_h}{1-{\nu_h}^2}\varepsilon_h + \frac{E_h \nu_h}{1-{\nu_h}^2}\varepsilon_H \tag{19}$$

$$\sigma_H = \alpha_h P_p + \frac{E_h}{E_v}\frac{V_v}{1-\nu_h}\left(\sigma_v - \alpha_v P_p\right) + \frac{E_h}{1-{\nu_h}^2}\varepsilon_H + \frac{E_h \nu_h}{1-{\nu_h}^2}\varepsilon_h \tag{20}$$

Where z is the vertical depth from ground level, g is the acceleration of gravity, ε_h and ε_H are the tectonic strains in the minimum and maximum stress direction respectively. All the rest of the variables were defined previously.

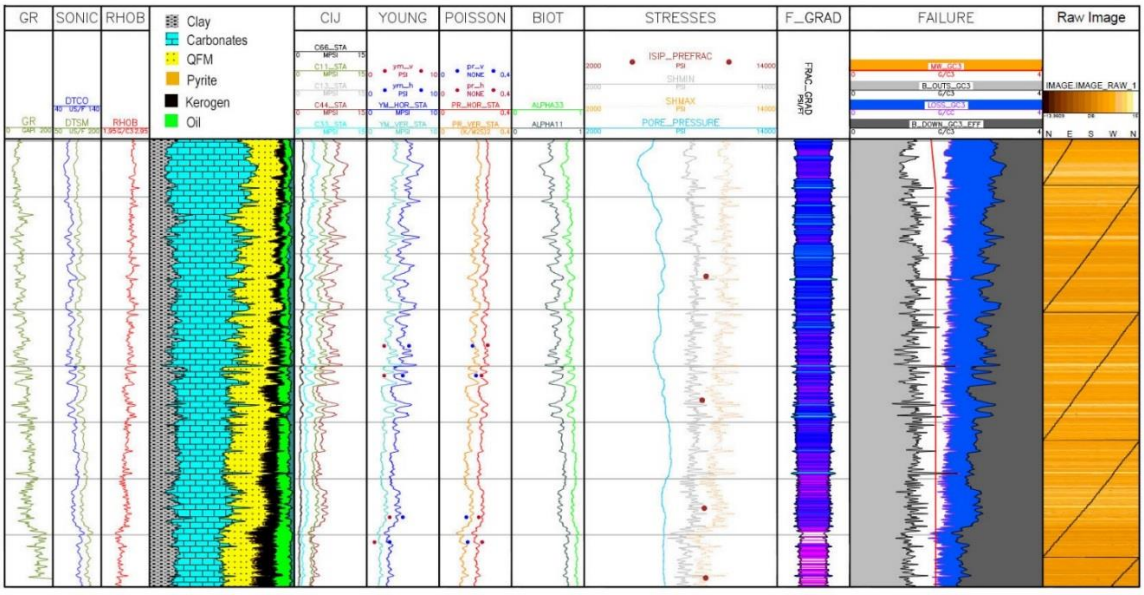

Figure 9: Results of the proposed model in one of the study wells, calculated elastic anisotropic moduli (columns 6 and 7) show a good calibration with triaxial tests for all the wells in the database. Minimum horizontal stress (track 9) are below ISIPs but in range and following the trends

Conclusions

There are important differences among the published methods to estimate far field stresses from well logs in unconventional plays. These differences are the product of different assumptions and simplifications. In addition, there are several empirical equations in use that have not been tested for the geological environments that we are trying to model here.

The fundamentals of the physical relationship between effective stress and compressional velocities have been well established, but, velocities also depend on matrix and fluid components, a normalization by these components need to be performed prior to the estimation of the effective stress. If, as in our case effective stress to velocity relationship is altered by overcompaction, a normalization need to be performed as well. Pore pressure estimation from effective stress needs a clear estimation of the value of Biot's alpha, since effective stress is sensitive to the combined effect of these variables.

Elastic anisotropy in highly laminated shales like the Vaca Muerta formation is high and needs to be considered for stress computation to obtain reasonable stress values. The usual main unknowns in 1D mechanical earth models are the maximum and minimum tectonic strains, since they cannot be measured. For this is important that all the rest of the parameter uncertainties are narrowed before estimating the strains. In our case, we have used pre-frac ISIPs as a calibration point for the minimum stress (realizing these values represent an upper boundary since they include the fracture net pressure). We have also used failure analysis as the preferred calibration tool for minimum and maximum tectonic strains for the wells where a wellbore image was available.

To reduce the uncertainties in the model our strategy was to batch running all the 40 wells of the model with the same parametrization, same coefficients and assumptions in order to interactively reduce the global error against the control points. Enough wells spread regionally are essential to gain confidence on parameter estimation using this approach.

Acknowledgments

We would like to thank Chevron Latin America and specially Chevron Argentina for allowing us publish the results of our work. We would like to thank José Adachi, Joris De Moor, Manuel Fantín, Dolores Vallejo and Carlos Paoletti for their important input and critical suggestions. We thank Juan Pablo Romanato and Mike Maneffa to give us the time and confidence to develop our models.

List of Symbols and Terms

TOC:	Total Organic Carbon
α:	*Biot's poroelastic constant*
ISIP:	*Instantaneous Shut-In pressure*
σ:	*Total stress*
σ':	*Effective stress*
Pp:	*Pore Pressure*
NCT:	*Normal Compaction Trend*
Vp:	*Compressional Velocity*
Vs:	*Shear velocity*
V_{max}	*Maximum compressional velocity before reversal*
σ_{max}:	*Maximum effective stress before reversal*
Vo:	*Velocity at cero effective stress*
φ:	*Porosity*
ρ:	*Density*
V_{clay}:	*Fraction Volume of clay minerals*
V_{carb}:	*Fraction Volume of carbonate minerals*
V_{qfm}:	*Fraction Volume of quartz, feldspars and micas*
V_{pyr}:	*Fraction Volume of pyrite*
V_{ker}:	*Fraction Volume of kerogen*
DT:	*Compressional sonic slowness in μs/ft*
Cij:	*Constants of the stiffness tensor*
E:	*Young modulus*
ν:	*Poisson Ratio*
K:	*Bulk modulus*
ε:	*Tectonic strains*

References

1. Athy, L. F., 1930. "Density, porosity and compaction of sedimentary rocks." American Association of Petroleum Geologists Bulletin, 14, 1–24.
2. Biot, M.A, 1941. General Theory of Three-Dimensional Consolidation. In Journal of Applied Physics, Volume 12, 155-164. Lancaster, Pennsylvania, USA.
3. Bowers, G.L. 1995. Pore Pressure Estimation from Velocity Data: Accounting for Overpressure Mechanisms Besides Undercompaction. IADC/SPE paper 27488 presented at the IADC/SPE Drilling Conference, Dallas, Texas, USA, 15-18 February 1994.
4. Burrus, J., 1998, Overpressure models for clastic rocks, their relation to hydrocarbon expulsion: a critical reevaluation, in Law, B.E., G.F. Ulmishek, and V.I. Slavin Eds., Abnormal pressures in hydrocarbon environments: AAPG Memoir 70, p. 35–63.
5. Crousse, L., Cuervo, S., Vallejo, D., Laurent, M., Fischer, T., & McCarty, D., 2015. Unconventional Shale Pore System Characterization in El Trapial Area, Vaca Muerta, Argentina. Unconventional Resources Technology Conference. doi:10.2118/178596-MS
6. Cuervo, S., Vallejo, M. D., Crousse, L., 2014. Caracterización integrada petrofísica y geomecánica de la formación Vaca Muerta en el área de El Trapial. In: Simposio de Recursos No Convencionales. IX Congreso Argentino de Exploración y Desarrollo de Hidrocarburos IAPG. Mendoza, Argentina.
7. Cuervo, S., Lombardo, E., Vallejo, D., Crousse, L., Hernandez, C., & Mosse, L., 2016. Towards a Simplified Petrophysical Model for the Vaca Muerta Formation. Unconventional Resources Technology Conference. San Antonio. Texas. URTEC-2016-243725
8. Davine, Paul E., 2014. Towards Understanding overpressure in a Basin with Burial and Uplift: Preliminary results of a Study Measuring Undercompaction with DT Logs. URTeC-1922841
9. Fantín, M., Crousse, L., Cuervo, S., Vallejo, D., Gonzalez Tomassini, F., Reijenstein, H., Lipinshki, C., 2014. Vaca Muerta Stratigraphy in Central Neuquén Basin: Imapct on Emergent Unconventional Projects. 1923793-MS URTeC.
10. Fjær E., R.M. Holt, P. Horsrud, A.M. Raaen & R. Risnes, 2008. Petroelum Related Rock Mechanics. 2nd Edition. Elsevier. ISBN: 978-0-444-50260-5
11. Frydman, M., Pacheco, F., Pastor, J., Canesin, F., Caniggia, J. and Davey, H., 2016. Comprehensive Determination of the Far-Field Earth Stresses for Rocks with Anisotropy in Tectonic Environment. SPE-180965-MS
12. Higgins, S. M., Goodwin, S. A., Donald, adam, Bratton, T. R., & Tracy, G. W., 2008. Anisotropic Stress Models Improve Completion Design in the Baxter Shale. Society of Petroleum Engineers. 115736-MS
13. Howell, J., Schwartz, E., Spalletti, L., Veiga, G. The Neuquén Basin: an overview. In: Veiga, G., Spalletti, L., Howell, J. & Schwartz, E. (Ed.), 2005. The Neuquén Basin, Argentina: A Case Study in Sequence Stratigraphy and Basin Dynamics. Geological Society, London.
14. Hower, J., E. V. Eslinger, M. E. Hower, and E. A. Perry, 1976, Mechanism of burial metamorphism of argillaceous sediment, 1: Mineralogical and chemical evidence: GSA Bulletin, 87, 725–737.
15. Huffman, A. and Bowers, G. Ed., 2001. Pressure Regimes in Sedimentary Basins and Their Prediction. AAPG Memoir 76. ISBN 158861333X.
16. Guzman, C., E. Cristallini, and G. Bottesi, 2007. Contemporary stress orientations in the Andean retroarc between 34S and 39S from borehole breakout analysis, Tectonics, 26, TC3016
17. Magara, K., 1978, Compaction and fluid migration: Practical petroleum geology: Development in Petroleum Science, 9 , Elsevier, Amsterdam, 343.
18. Mavko, G., Mukerji, T., Dvorkin, J. The Rock Physics Handbook, Second Edition., 2009. Cambridge University Press. ISBN-13 978-0-521-86136-6
19. Mosquera, A., Ramos, V. A., 2005. Interplate Foreland Deformation in the Neuquen Embayment. Search and Discovery Article #30035. AAPG Annual Convention, Calgary, Alberta.
20. Rimedio, M., Shannon, C., Monti, L., Lerza, A., Roberts, M., Quiroga, J., 2015. Interference Behavior Analysis in Vaca Muerta Shale Oil Development, Loma Campana Field. Argentina. 2154850-MS URTeC.
21. Sayers, C. M., Smit, T. J. H., van Eden, C., Wervelman, R., Bachmann, B., Fitts, T., Bingham, J., McLachlan, K., Noeth, S., Mandhiri, D., 2003. Use of Reflection Tomography to Predict Pore Pressure In Overpressured Reservoir Sands. Society of Exploration Geophysicists. SEG Conference Paper.
22. Sayers, C., 2010. Geophysics under stress: Geomechanical applications of seismic and borehole acoustic waves. EAGE Distinguished Instructor Short Course. Distinguished Instructor Series, Nro 13.
23. Scasso, R., Alonso, M., Lanés, S., Villar, H., Laffitte, G., 2005. Geochemistry and petrology of a Middle Tithonian limestone-marl rythmite in the Neuquén Basin, Argentina: depositional and burial history (207-229). In: Veiga, G., Spalletti, L., Howell, J. & Schwartz, E. Eds. 2005. The Neuquén Basin, Argentina: A Case Study in Sequence Stratigraphy and Basin Dynamics. Geological Society, London, Special Publications.
24. Schmidt, N., Alonso, J., Giusiano, A., Lauri, C., Sales, T., 2014. El shale de la formación Vaca Muerta: integración de datos y estimación de recursos de petróleo y gas asociado, Provincia de Neuquén. In: Simposio de Recursos No Convencionales. IX Congreso Argentino de Exploración y Desarrollo de Hidrocarburos IAPG. Mendoza, Argentina.
25. Singh, A., Bertoncello, A., Brigaud, F., & Foulon, D., 2016. Early Delineation of Productive Areas in Unconventional Plays Using Uplift Intensity- a Utica Example. Unconventional Resources Technology Conference. URTEC-2016-2430161

26. Suarez-Rivera, R., Deenadayalu, C., Chertov, M., Hartanto, R. N., Gathogo, P., & Kunjir, R., 2011. Improving Horizontal Completions on Heterogeneous Tight-Shales. Society of Petroleum Engineers. 146998-MS.
27. Suarez-Rivera, R., & Fjaer, E., 2012. How Important is the Poroelastic Effect to Completion Design On Tight Shales? American Rock Mechanics Association. 46th US Rock Mechanics / Geomechanics Symposium.
28. Swarbrick, R., Osborne, M., Yardley, G., 2002. Comparison of Overpressure Magnitude Resulting from the Main Generating Mechanisms. in A. R. Huffman and G. L. Bowers, eds., Pressure regimes in sedimentary basins and their prediction: AAPG Memoir 76, p. 1–12.
29. Terzaghi, K., 1936. "Stress distribution in dry and saturated sand above a yielding trap door". In: Proc. Int. Conference on Soil Mechanics and Foundation Engineering, Cambridge, MA, vol. 1, pp. 307–311.
30. Uliana, M., Legarreta, L., 1993. Hydrocarbons Habitat in a Triassic to Cretaceous Sub-Andean Settings: Neuquén Basin, Argentina. Journal of Petroleum Geology. Vol 16 (4), pp. 397-420.